Articles

A Theoretical Study of Syndiospecific Styrene Polymerization with Cp-Based and Cp-Free Titanium Catalysts. 2. Mechanism of Chain-End Stereocontrol

Gianluca Minieri,[†] Paolo Corradini,[†] Gaetano Guerra,[‡] Adolfo Zambelli,[‡] and Luigi Cavallo*,[†]

Dipartimento di Chimica, Università di Napoli, Complesso Monte S. Angelo, Via Cintia, Napoli, I-80126, Italy; and Dipartimento di Chimica, Università di Salerno, Via Allende, Baronissi (SA), I-84081, Italy

Received December 20, 2000; Revised Manuscript Received April 27, 2001

ABSTRACT: A theoretical study of the mechanism of chain-end stereocontrol in the syndiospecific polymerization of styrene with models based on the $CpTi^{III}CH(Ph)CH_3^+$ species is presented. Independent of the chirality of styrene coordination, low-energy transition states are always characterized by interactions of the aromatic group of the last enchained unit with the metal atom. However, the most stable transition state leads to formation of a syndiotactic diad, and it is favored by 6 kJ mol^{-1} with respect to the most stable transition state which leads to an isotactic diad. According to our calculations, the transition state which leads to a syndiotactic diad is favored because the smallest substituent on the C_α atom of the chain, the H atom, can be pointed toward the Cp ligand. On the other hand, the transition state which leads to an isotactic diad is of higher energy because one group between the aromatic ring on the C_α atom of the growing chain, or the C_β and following groups of the growing chain, must be oriented toward the Cp ring. In agreement with experiments, models of the type $Cp^*Ti^{III}CH(Ph)CH_3^+$ and $(benzene)Ti^{II}CH(Ph)CH_3^+$ are calculated to be more stereoselective than $CpTi^{III}CH(Ph)CH_3^+$, since the transition states leading to a syndiotactic diad are favored by 16 and 13 kJ mol^{-1} with respect to the transition states leading to an isotactic diad.

Introduction

Syndiotactic polystyrene is a new polymeric material, which was discovered in 1986 by Ishihara and co-workers.[1,2] The high crystallization rate and the high melting point, 270 °C,[1] make syndiotactic polystyrene a crystalline engineering thermoplastic material of industrial relevance.[3−8]

Highly syndiotactic polystyrene (fraction of the *rrrrrr* heptad >94%)[2] can be obtained with several soluble titanium, and to a less extent zirconium, compounds. The best performances are obtained with monocyclopentadienyl compounds of titanium, as $CpTiX_3$ or Cp^*TiX_3 ($Cp = \eta^5$-C_5H_5; $Cp^* = \eta^5$-C_5Me_5 or another substituted Cp ligand; X = F, Cl)[9−15] activated by methylalumoxane (MAO) or $B(C_6F_5)_3$.[16,17] Cp-free compounds as $Ti(CH_2Ph)_4$ and $Ti(OR)_4$ (R = alkyl, aryl) are also moderately active.[18] In short, many soluble titanium compounds can be used as precatalyst, but it is worthwhile to note that titanocene compounds, quite active in the polymerization of 1-olefins,[19] are among the less active species for styrene polymerization[2,20] and that zirconium compounds are generally much less active than the analogous titanium compounds.[21]

The nature of the real active species in styrene syndiotactic polymerization is still debated in the literature.[22−31] However, on the basis of kinetic, ESR, and NMR studies, Zambelli and co-workers proposed that the real active species could be of the type $CpTi^{III}P^+$ (P = polymeryl), for the Cp-based systems, and of the type $(arene)Ti^{II}P^+$ for the Cp-free systems. In the latter case, the Cp ring would be replaced by an arene neutral η^6-ligand, affording a cationic Ti^{II} complex.[32−34] In a previous paper, we have performed density functional calculations on the elementary steps of the mechanism of styrene polymerization using as models Ti^{III} species of the type $CpTi^{III}CH_2P^+$, and Ti^{II} species of the type $(benzene)Ti^{II}CH_2P^+$, and $CpTi^{II}CH_2P$.[35] The main results of this study supported the proposal that species like $CpTi^{III}CH_2P^+$ are indeed involved in styrene polymerization with Cp-based systems, and that species like $(benzene)Ti^{II}CH_2P^+$ could be the ones active with Cp-free systems. Moreover, our calculations indicated that species like $CpTi^{III}CH_2P^+$ should be quite more active that species like $(benzene)Ti^{II}CH_2P^+$, which is in agreement with the experimentally observed higher activity of Cp-based systems relative to Cp-free systems.

Although there is some debate about the exact nature of the species active in polymerization, NMR experiments have clearly indicated that this polymerization reaction occurs through a Ziegler−Natta type polyinsertion mechanism. In particular, these experiments have shown the following: (i) the insertion occurs through cis opening of the monomer double bond;[36] (ii)

* Corresponding author. E-mail: cavallo@chemistry.unina.it.
[†] Università di Napoli.
[‡] Università di Salerno.

10.1021/ma002163d CCC: $20.00
Published on Web 06/28/2001

the regiochemistry of styrene insertion is secondary and highly regioselective;[37,38] (iii) the stereoselectivity of the insertion step is controlled by the chirality of the growing chain-end. This is clearly indicated by the analysis of the stereochemical composition of the syndiotactic polymers, which shows the presence of *rmr* tetrads and the substantial absence of *rmm* tetrads.[21,39,40] Although highly stereoselective, the syndiotacticity of the polystyrene samples is somewhat dependent from the particular catalyst used. With simple $CpTiCl_3$/MAO, the probability of formation of a *r* diad, P_r, goes from ∼1 to 0.92, as the temperature goes from −17 to +90 °C, which correspond to a fraction of *rrr* tetrads equal to ∼1 and 0.79, respectively.[40] With Cp-free systems of the type $Ti(CH_2Ph)_4$/MAO, P_r is close to 0.98 in the range 50−90 °C, while better results are obtained with Cp^*TiCl_3/MAO, for which P_r is substantially 1 even at 90 °C. It is worthwhile to note that such a high stereoselectivity in chain-end stereocontrolled polymerizations was unprecedented, and the origin of such an exquisite stereocontrol is still unclear.

While many experimental studies have provided substantial information on the polymerization mechanism, to date almost nothing has been done from a theoretical point of view. This is in sharp contrast to the considerable amount of computational studies which have contributed to the comprehension of even fine details of site and chain-end controlled mechanisms of stereoselectivity in the 1-olefins polymerizations with both early and late transition metals.[19,41,42] These studies have shown that when a substantial site-stereocontrol is calculated for primary propene insertion, this can be rationalized by the so-called mechanism of *chiral orientation of the growing chain*. According to this mechanism, the growing chain is forced to assume a chiral orientation by nonbonded interactions with the chiral framework of the catalyst. This chiral orientation of the growing chain, in turn, selects between the two prochiral enantiofaces of the incoming monomer. Instead, the chain-end stereocontrol usually leads to lower stereoselectivities,[43−45] and for this reason the corresponding catalytic systems have not reached industrial relevance for propene homopolymerization. However, some of them are widely used for propene copolymerization with ethene. In particular, the syndiospecific chain-end controlled polymerization of propene with V-based catalysts is known since the 1960s. For these systems, it has been shown that propene insertion is scarcely regioselective and that the stereoselective step is secondary propene insertion into a secondary growing chain.[46−48] A molecular mechanics study of these systems suggested that the chirality of the last C atom of the growing chain could induce a preferential Λ or Δ configuration at the octahedrally coordinated V atom which, in turn, would select the propene prochiral face which minimized steric interactions with the other V ligands.[49]

With regard to the syndiospecific styrene polymerization, attempts to correlate the experimental data with steric models are due to some of us and to Porri et al.[50−52] In particular, Porri and Zambelli independently proposed that the growing chain could be substantially σ-bonded to the metal at the transition state, although some atoms of the aromatic group of the last inserted unit could interact with the metal, and that the chirality of the last C atom of the chain would induce a preferred chirality at the metal atom. This induced chirality at the metal would select the enantioface of the incoming styrene monomer in order to reduce steric interactions between the growing chain, the monomer, and the ancillary Cp ligand.

To test for these hypotheses, in the wake of our previous study of the elementary steps which compose the propagation cycle,[35] we decided to make a density functional study about the origin of stereoselectivity in the syndiospecific polymerization of styrene with both Cp-free and Cp-based catalysts. In particular, we investigated possible geometries of the transition state of the insertion step. The basic features of these transition states were determined previously, and they will be the starting point for the calculations presented here. The main difference with respect to the previous study is the presence of a chiral growing chain. In particular, we will present results on the stereoselectivity of styrene insertion on the $CpTi^{III}CH(Ph)CH_3^+$ and $Cp^*Ti^{III}CH(Ph)CH_3^+$ active species, which are representative of Cp-based systems, and on the $(benzene)Ti^{II}CH(Ph)CH_3^+$ active species, as representative of Cp-free systems.

Models and Methods

The models used to investigate the propagation mechanism are composed by monometallic cationic species. These models comprise a Ti atom in the oxidation state III with a spectator Cp ligand coordinated or a Ti atom in the oxidation state II with a spectator C_6H_6 ligand coordinated. The C_6H_6 is used to simulate a neutral η^6-ligand. Furthermore, a growing chain simulated by the chiral $-CH(Ph)CH_3$ group will be coordinated to the metal. Coordination and insertion of a styrene molecule to these systems will be considered.

The main elements of chirality that are relevant for the present study are briefly recalled here. First of all, upon coordination the prochiral styrene molecule gives rise to nonsuperimposable *re* and *si* coordinations.[53] A second element of chirality is the configuration of the tertiary carbon atom of the growing chain nearest to the metal atom, and the Cahn−Ingold−Prelog *R*, *S* nomenclature will be used. In this study, the growing chain will be modeled with the chiral $-CH(Ph)CH_3$ group of *R* configuration, which stems from insertion of a *re*-coordinated styrene. For this reason, we will refer to the $-CH(Ph)CH_3$ group of *R* configuration as the *re*-ending chain. Finally, also the pseudotetrahedral metal atom is chiral in these systems, and the extension of the CIP nomenclature to organometallic compounds, as proposed by Stanley and Baird, will be used here.[54] In order of priority, the four different substituents used to define the chirality at the pseudotetrahedral metal atom are as follows: (i) the center of mass of the ancillary aromatic Cp or C_6H_6 ligand, (ii) the center of mass of the two C atoms of the aromatic ring of the styrene molecule which are coordinated to the metal, (iii) the center of mass of the monomer double bond, and (iv) the C_α atom of the growing chain. Within this choice, *R* is the configuration at the metal atom in structures **1-syndio**, **2-syndio**, and **3-syndio** of Figure 2, while it is *S* in structures **1-iso**, **2-iso**, and **3-iso** of Figure 2.

Stationary points on the potential energy surface were calculated with the Amsterdam Density Functional (ADF) program system release 2.3.0[55] developed by Baerends et al.[56−59] The electronic configuration of the molecular systems were described by a triple-ζ basis set on titanium for 3s, 3p, 3d, and 4s, plus one 4p function (ADF basis set IV).[55] Double-ζ STO basis sets were used for carbon (2s, 2p) and hydrogen (1s), augmented with a single 3d and 2p function, respectively (ADF basis set III).[55] The inner shells on titanium (including 2p) and carbon (1s) were treated within the frozen core approximation. Energetic and geometries were evaluated by using the local exchange-correlation potential by Vosko et al,[60] augmented in a self-consistent manner with Becke's exchange gradient correction[61] and Perdew's correlation gradient correction.[62,63] An unrestricted formalism was used for all species

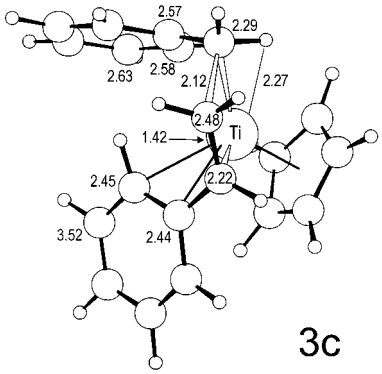

Figure 1. Geometry of the lowest energy transition state for insertion of styrene on the $CpTi^{III}CH_2Ph^+$ species, in which the growing chain is simulated with the achiral $-CH_2Ph$ group. The numbers close to the C atoms represent the distance of these atoms from the metal. All distances are reported in Å.

with unpaired electrons. To check for the real nature of the most favored transition states, we performed frequency calculations on the lowest energy transition state geometries leading to a syndio- and to an isotactic diad with the $CpTi^{III}$-$CH(Ph)CH_3^+$ system. These calculations were also used to evaluate the vibrational zero point energy and thermodynamic corrections, according to standard textbook procedures.[64]

The energy differences with inclusion of solvent effects were calculated by correcting the gas-phase energy with the use of the conductor-like screening model, COSMO, of Klamt and Schüürmann,[65] as implemented in the ADF package.[66] The calculations of the solvation energies were performed with a dielectric constant $\epsilon = 2.38$ to represent toluene as solvent. The van der Waals surface was used to build the cavity containing the molecule, and the standard radii H = 1.29 Å and C = 2.00 Å, of Klamt and Schüürmann were used.[65] For Ti, we used a radius of 2.30 Å, as proposed by Ziegler and coworkers.[67] The calculations of energies including solvation effects were performed as single point calculations on the gas-phase optimized geometries. The 2000 release of the ADF package was used for these calculations.[68]

Results and Discussion

Transition States for the Insertion Reaction. The following calculations will be based on geometries having the same basic features we found for the most favored transition state for styrene insertion into the Ti−C bond of the $CpTi^{III}CH_2P^+$ species discussed in our previous paper and labeled **3c**.[35] For the sake of readability, the geometry of this transition state is reported in Figure 1, and it is briefly discussed. The growing chain, modeled by the $-CH_2Ph$ group, is substantially σ-bonded to the metal atom, since a short Ti−CH_2-(benzyl) distance is present. However, some of the C atoms of the aromatic ring of the benzyl group are at distances of coordination from the metal atom. This suggests that a stabilizing interaction occurs between the titanium and the phenyl ring of the benzyl group. As for the styrene monomer, it is clearly cis-η^4-coordinated to the metal, since only the two olefinic C atoms, the *ipso*-C and one of the *ortho*-C atoms of the aromatic ring are at distances of coordination from the metal atom. The overall structure presents the classical four-centers geometry that characterizes olefins polymerization reactions. The Ti−CH_2(benzyl), Ti−CH(styrene), and CH_2(styrene)−CH_2(benzyl) distances are very close to the analogous distances in the transition state for olefin polymerization with group 4 metallocenes. The torsional angle Ti−CH(styrene)−CH_2(styrene)−CH_2-(benzyl) assumes a value close to −8°, which indicates

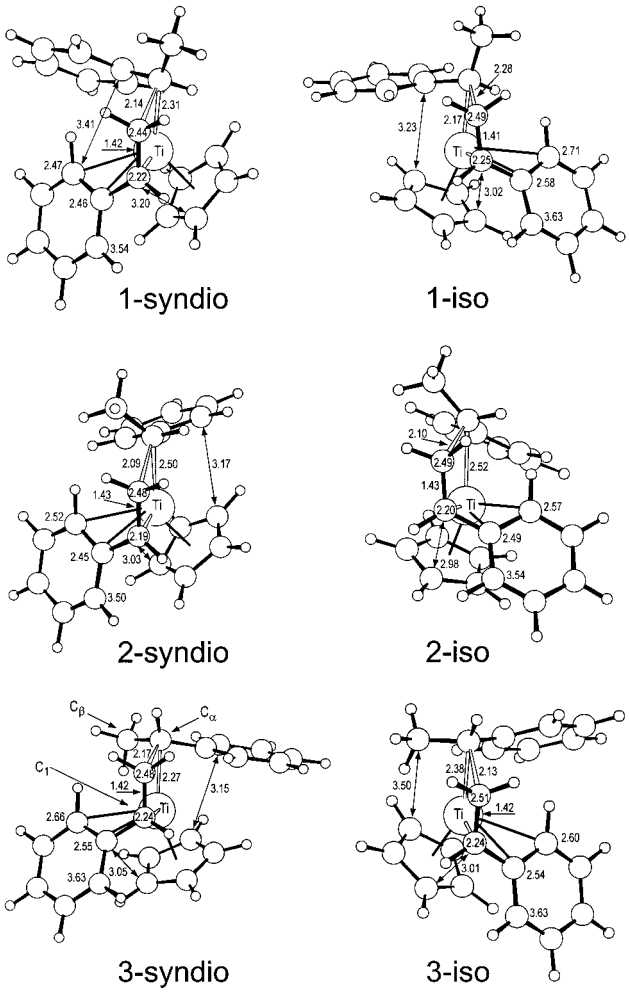

Figure 2. Geometries of the transition states for insertion of styrene on the $CpTi^{III}CH(Ph)CH_3^+$ species, in which the chiral $-CH(Ph)CH_3$ group is used to simulate a *re*-ending growing chain. The numbers close to the C atoms represent the distance of these atoms from the metal. All distances are reported in Å. Structures **1**−**3-syndio** are characterized by a *re*-ending chain, a *si*-coordinated monomer and a *R* configuration at the metal atom. They mainly differ in the value assumed by the θ_1 torsional angle. Instead, structures **1**−**3-iso** are characterized by a *re*-ending chain, a *re*-coordinated monomer, and a *S* configuration at the metal atom. They mainly differ in the value assumed by the θ_1 torsional angle. It is worthwhile to note that structures **1**−**3-iso** are diastereoisomers of structures **1**−**3-syndio**, since they are characterized by the same configuration of the chain-end, but they differ in the configuration of the styrene coordination and of the metal atom.

an almost planar transition state geometry. Moreover, an adjuvant α-agostic interaction of the Ti atom with a H atom of the benzyl CH_2 groups is present. It is worthwhile to note that approach of the styrene aromatic ring to the Ti atom occurs in a relatively uncrowded sector, since the aromatic ring of the styrene and the Cp ring are on opposite sides of the plane of the four-centers transition state.

The model shown in Figure 1 presents a styrene monomer coordination suitable for secondary insertion (by using the notation used for models for olefin polymerization,[41,49] the dihedral angle θ_0 relative to the orientation of the monomer double bond with respect to the bond between metal and growing chain is nearly equal to 180°). Moreover, a given chirality of styrene monomer coordination (*re* or *si*) is associated with a given chirality at the pseudotetrahedral metal center

Scheme 1. Possible Mechanism of Stereospecificity

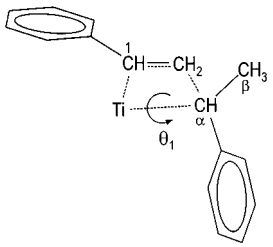

(*S* or *R*, respectively). This occurs independent of the chemical structure as well as of the chirality of the growing chain.

The growing chain of structure **3c**, however, is achiral, and to discuss a possible mechanism of stereoselectivity, we have to introduce a chiral growing chain. The combination of the chirality of the growing chain-end with the chirality of monomer coordination (and the associated chirality at the metal) originates diastereoisomeric situations of, possibly, different energy. The achiral $-CH_2Ph$ benzyl group is thus made chiral by substituting one of the H atoms of the CH_2 group with a methyl group. The *R* or *S* configuration of the resulting $-CH(Ph)CH_3$ group depends on which particular H atom has been substituted by a methyl group. For clarity of presentation, to build the thus arising diastereoisomeric transition states we considered **3c** and its mirror image to have the $-CH(Ph)CH_3$ group of the same configuration *R*, in both structures. As explained in the Models and Methods section, we will refer to it as the *re*-ending chain, since *R* is the configuration of the $-CH(Ph)CH_3$ group which stems from insertion of a *re*-coordinated styrene.

Starting from structure **3c** and considering both the *re*- and *si*-styrene enantiofaces, we calculated the rotational profiles around the angle θ_1 (defined as the torsional angle $C_1-Ti-C_\alpha-C_\beta$, see Scheme 1) in the range 0−180° with increments of 60°. At each increment we optimized the energy with respect to all the degrees of freedom, with exception of the θ_1 angle and of the distance between the two C atoms that will form the new C−C bond which was fixed at 2.15 Å. All the structures that were found to be within a threshold of 30 kJ mol^{-1}, with respect to the most stable structure, were subsequently used as the starting point for a full transition state search. The so-localized transition states are reported in Figure 2. Structures **1-syndio**, **2-syndio**, and **3-syndio** with a *si*-coordinated styrene (and *R* configuration at metal center), are characterized by values of θ_1 equal to +35, −74, and −127°, while their diastereoisomeric structures **1-iso**, **2-iso**, and **3-iso** with a *re*-coordinated styrene (and *S* configuration at metal center), are characterized by values of θ_1 equal to +15, −73, and −112°, respectively. All these structures are still characterized by a strong σ-bond interaction between the growing chain and the Ti atom, while the styrene molecule still is cis-η^4-coordinated. Moreover, all of them retain the classical four-centers geometry that characterizes the transition state of olefins polymerization reactions. In fact, the Ti−CH(benzyl), Ti−CH(styrene), and CH_2(styrene)−CH(benzyl) distances are very close to the analogous distances in **3c**, while the torsional angle Ti−CH(styrene)−CH_2(styrene)−CH(benzyl) assumes values in the range ±10°, which indicates an almost planar transition state geometry. Of relevance is the fact that all these low-energy structures present the aromatic ring of the growing chain somewhat coordinated to the metal atom. The higher energy of the structures not shown here is a consequence of the loss of the energy stabilization due to even partial coordination of the aromatic ring of the growing chain to the metal.

With regard to structures which would lead to a syndiotactic diad, that is with a *si*-coordinated monomer, the situation with θ_1 equal to 35°, **1-syndio**, is the most stable, since structures with θ_1 equal to −74 and −127°, **2-syndio** and **3-syndio**, are 8 and 15 kJ mol^{-1} higher in energy, respectively. Structure **1-syndio** presents a relative disposition of the growing chain, of the monomer, and of the Cp ring very similar to that of the achiral structure **3c**. The aromatic rings of both the growing chain and of the monomer are far from the Cp ring. The shortest distance between C atoms belonging to different groups is 3.2 Å, and it occurs between a C atom of the styrene with a C atom of the Cp ring. The shortest distance between aromatic C atoms of the growing chain and of the styrene is 3.4 Å. Moreover, the methyl group used to simulate the C_β of the *re*-ending growing chain develops far from the coordination sphere of the metal atom presenting a *S* configuration, and repulsive interactions with other ligands are negligible. Instead, in structures **2-syndio** and **3-syndio**, short distances (∼3.0 Å) occur between the Cp ring and the styrene, as well as between the Cp ring and the growing chain.

With regard to structures which would lead to an isotactic diad, that is with a *re*-coordinated monomer, the situation with θ_1 equal to −112°, **3-iso**, is the most stable since structures with θ_1 equal to +15 and −73° **1-iso** and **2-iso**, are 3 and 17 kJ mol^{-1} higher in energy, respectively. Structure **3-iso** presents a relative disposition of the growing chain, of the monomer, and of the Cp ring very similar to that of structures **3c** and **1-syndio**. However, in **3-iso**, the methyl group used to simulate the following of the *re*-ending growing chain develops into the coordination sphere of the metal atom which presents a *S* configuration, and some steric repulsive interactions with other ligands, the Cp ring in particular, are present. As a consequence, the C_1 atom of the monomer molecule is at a short distance (3.0 Å) from the Cp ring. In structures **1-iso** and **2-iso**, beside the Cp ring and the styrene, short distances (∼3.0 Å) occur between the Cp ring and the aromatic ring of the growing chain as well.

The higher steric stress of structure **3-iso** relative to that of structure **1-syndio** is also suggested by the higher deviation of **3-iso** from the parent structure **3c**, with respect to the deviation of **1-syndio** from **3c**. In fact, the rms deviations of **3-iso** and **1-syndio** from **3c**, obtained by superimposing the heavy atoms skeleton of **3-iso** and **1-syndio** to the skeleton of **3c**, amount to 0.22 and 0.07 Å, respectively. Moreover, as shown by the overlaps reported in Figure 3, it is clear that deformations in **3-iso** are most localized around the Cp ring and the C_α of the growing chain, further indication of repulsive interactions between the Cp ring and the methyl group.

Of paramount relevance, however, is the fact that **1-syndio** is the most stable structure independently of the chirality of coordination of the monomer (see Table 1). In fact, structures with a *re*-coordinated monomer **1-iso**, **2-iso**, and **3-iso**, are 7, 21, and 4 kJ mol^{-1} above **1-syndio**, respectively. In short, formation of a syndiotactic diad is favored. The $\Delta\Delta E^{\ddagger}$ preference, for the

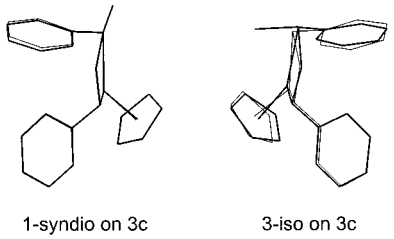

Figure 3. Schematic superposition of structures **1-syndio** and **3-iso** with a chiral growing chain, to the parent transition state **3c** with an achiral growing chain, parts A and B, respectively.

Table 1. Relative Energies of the Most Important Transition States

structure	energy (kJ mol^{-1})
1-syndio	0
2-syndio	8
3-syndio	15
1-iso	7
2-iso	21
3-iso	4
Cp*-syndio	0
Cp*-iso	16
C_6H_6-syndio	0
C_6H_6-iso	13

formation of a syndiotactic diad we have calculated, is equal to 4 kJ mol^{-1}. Inclusion of the vibrational zero point energy and of the $-T\Delta S$ contribution, evaluated at 298 K and 1 atm, leads to an increased $\Delta\Delta G^{\ddagger}$ of 8 kJ mol^{-1} in the gas phase, whereas inclusion of solvent effects slightly decreases the gas phase $\Delta\Delta G^{\ddagger}$ to the value of 6 kJ mol^{-1} for $\Delta\Delta G^{\ddagger}$ in solution. The calculated $\Delta\Delta G^{\ddagger}$ values are in good agreement with the experimental difference between the apparent energies of activation leading to *r* and *m* diads, ΔE_a,[69] which has been determined to be 7−8 kJ mol^{-1}.[40]

From a geometrical viewpoint, it is worthwhile to note that the most preferred structure **1-syndio** is characterized by a θ_1 value, |35|°, quite similar to the θ_1 values, |∼60|°, we calculated to be the preferred ones in the polymerization of propene with group 4 metallocenes.[19,41] In the case of chiral group 4 metallocenes, the chiral framework provided by the ligand forces the growing chain to assume a chiral orientation which, in turn, selects the chirality of the incoming propene molecule.

In this case, instead, a preferential configuration at the metal atom is induced in order to avoid repulsive interactions between the various ligands. In the case of a *re*-ending chain, the *R* configuration at the metal atom (which is associated with a *si*-coordinated styrene) is favored because the smallest substituent on the C_α atom of the chain, the H atom, can be pointed toward the Cp ligand, as occurs in **1-syndio**. On the other hand, in the case of a *re*-ending chain, the *S* configuration at the metal atom (which is associated with a *re*-coordinated styrene) is of higher energy because one group between the aromatic ring on the C_α atom of the growing chain, or the C_β and following of the growing chain, must be oriented toward the Cp ring. As a consequence, it is reasonable that the most favored situation is the one with the smaller methyl group pointed toward the Cp ligand, as occurs in **3-iso**. The unfavored *S* configuration at the metal atom would generate a stereomistake (*m* diad, rather than a *r* diad) because it would lead to the insertion of the *re* enantioface of the incoming styrene molecule.

A similar model, was proposed to explain the syndiospecificity in the secondary propene polymerization

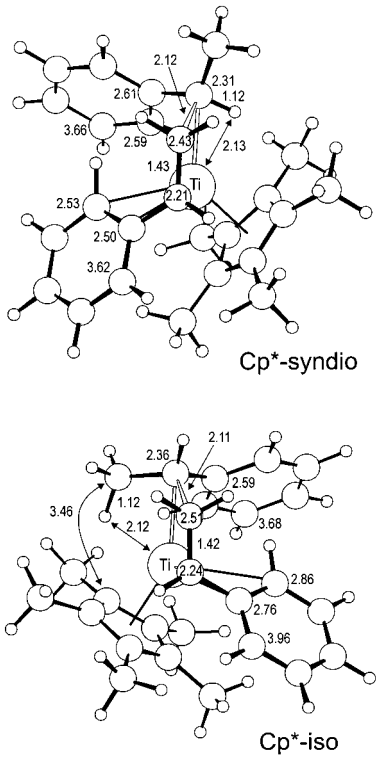

Figure 4. Geometries of the transition states for insertion of styrene on the Cp*Ti^{III}CH(Ph)CH$_3^+$ species, in which the chiral −CH(Ph)CH$_3$ group is used to simulate a *re*-ending growing chain. The numbers close to the C atoms represent the distance of these atoms from the metal. All distances are reported in Å.

of propene with soluble V compounds.[49] It was suggested that the chirality at the C_α of the growing chain induces a favored Λ or Δ configuration at the octahedrally coordinated V atom which, in turn, would select the propene prochiral face which minimized steric interactions with the other V ligands. Moreover, it is also worthwhile to note that the most favored structure has strong similarities (σ-bonding of the growing chain, η^4-coordination of the monomer, preferential chirality at the metal atom induced by the chirality of the C_α of the chain) with hypotheses independently presented by Porri and Zambelli to explain the syndiospecificity of such systems.[51,52]

Finally, we decided to test the model by calculating the $\Delta\Delta E^{\ddagger}$ between **1-syndio** and **3-iso** when the Cp ligand is replaced by the bulkier Cp* ligand, or when the active species is a cationic Ti^{II} species of the type (benzene)Ti^{II}P$^+$. The latter, is the species proposed to be the active one in the syndiospecific styrene polymerization with Cp-free catalysts, a proposal also supported by our previous calculations.[35] The transition states relative to the system with the Cp* ligand, **Cp*-syndio** and **Cp*-iso**, are reported in Figure 4, while the transition states relative to the cationic Ti^{II} system with benzene as ligand, **C_6H_6-syndio** and **C_6H_6-iso**, are reported in Figure 5.

The structures of Figures 4 and 5 have geometries quite similar to those of **1-syndio** and **3-iso** and hence will be not discussed. From an energetical point of view, however, a higher preference in favor of the transition state leading to the syndiotactic diad is calculated both for the system with the bulkier Cp* ligand and for the Ti^{II} active species with benzene as ligand, with respect to the system with a Cp ligand. In fact, **Cp*-syndio** and

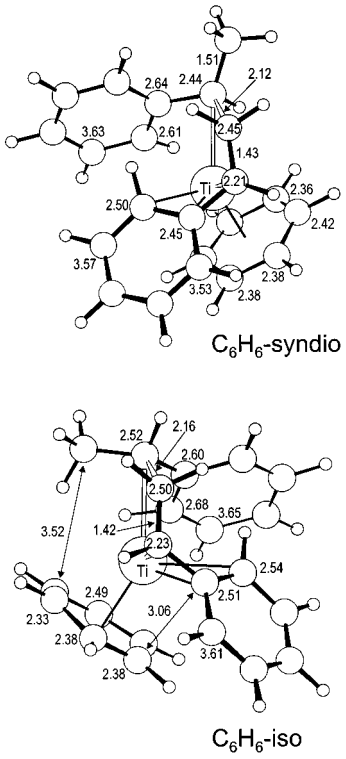

Figure 5. Geometries of the transition states for insertion of styrene on the (benzene)$Ti^{II}CH(Ph)CH_3^+$ species, in which the chiral $-CH(Ph)CH_3$ group is used to simulate a *re*-ending growing chain. The numbers close to the C atoms represent the distance of these atoms from the metal. All distances are reported in Å.

C_6H_6-syndio are favored by 16 and 13 kJ mol^{-1} relative to **Cp*-iso** and **C_6H_6-iso**, respectively.

The higher stereoselectivity of these systems is due to increased repulsive interactions between the methyl group of the benzyl-type growing chain, and the bulkier Cp* or benzene ligand, in **Cp*-iso** and **C_6H_6-iso** with respect to **3-iso**, and to the slightly more compact geometry of the Ti^{II} system with benzene as ligand. The higher stereoselectivity we calculated for these latter systems with respect to the Cp-based system, is in good agreement with the experimental results. In fact, the probabilities of *r* enchainment, P_r, experimentally found by Zambelli and co-workers at 90 °C, are equal to 0.92, 0.98, and ~1, for the catalytic systems $CpTiCl_3$/MAO, $Ti(CH_2Ph)_4$/MAO and Cp^*TiCl_3/MAO, respectively.[40]

Conclusions

In this paper, we have presented a DFT study of a possible mechanism of stereoselectivity in the syndiospecific polymerization of styrene. The main conclusions can be summarized as follows:

(i) Independent of the chirality of styrene coordination, low-energy transition states are always characterized by interactions of the aromatic group of the last enchained unit with the metal atom. Transition states which do not have interactions between the aromatic group of the last enchained unit and the metal atom are at least 30 kJ mol^{-1} higher in energy.

(ii) The most stable transition state leads to the formation of a syndiotactic diad, since it corresponds to *si*-styrene insertion on a *re*-ending growing chain and it is favored by 6 kJ mol^{-1} with respect to the insertion of a *re*-coordinated styrene on a *re*-ending growing chain. According to our calculations, the chirality of monomer coordination induces a preferential chirality at the metal atom in order to avoid repulsive interactions between the various ligands. In particular, a *re*-coordinated styrene induces a *S* configuration at the metal atom, while a *si*-coordinated one induces a *R* configuration. In the case of a *re*-ending chain, the diastereoisomeric transition state with a *R* configuration at the metal is favored because the smallest substituent on the C_α atom of the chain, the H atom, can be pointed toward the Cp ligand, as occurs in **1-syndio**, whereas the diastereoisomeric transition state with a *S* configuration at the metal is of higher energy because one group between the aromatic ring on the C_α atom of the growing chain, or the C_β and following of the growing chain, must be oriented toward the Cp ring, as occurs in **3-iso**. Finally, it is worthwhile to note that the most preferred structure **1-syndio** is characterized by a relative geometrical arrangement of monomer and growing chain very close to those generally assumed for olefin polymerization with group 4 metallocenes.

(iii) In agreement with experiments, calculations on models of the type $Cp^*Ti^{III}CH(Ph)CH_3^+$ and (benzene)$Ti^{II}CH(Ph)CH_3^+$ indicated that these systems are more stereoselective than $CpTi^{III}CH(Ph)CH_3^+$, since the transition states leading to a syndiotactic diad are favored by 16 and 13 kJ mol^{-1} with respect to the transition states leading to an isotactic diad. The higher stereoselectivity of these systems is due to increased repulsive interactions between the methyl group of the benzyl-type growing chain, and the bulkier Cp* or benzene ligand, in **Cp*-iso** and **C_6H_6-iso** with respect to **3-iso**. Finally, in agreement with experiments models of the type (benzene)$Ti^{II}CH(Ph)CH_3^+$ are calculated to be more stereoselective than $CpTi^{III}CH(Ph)CH_3^+$, and slightly less stereoselective than $Cp^*Ti^{III}CH(Ph)CH_3^+$. This is a further support to the proposal that the active species in Cp-free catalysts could be of the type (arene)-$Ti^{II}P^+$ (P = polymeryl).

Acknowledgment. We thank Prof. Porri, Polytechnic of Milano and our colleagues at the University of Salerno for useful discussions. This project has been supported by MURST of Italy, Grants PRIN-1998 and PRIN-2000, and by Basell Polyolefins.

References and Notes

(1) Ishihara, N.; Seimiya, T.; Kuramoto, M.; Uoi, M. *Macromolecules* **1986**, *19*, 2464.
(2) Ishihara, N.; Kuramoto, M.; Uoi, M. *Macromolecules* **1988**, *21*, 3356.
(3) Review: Tomotsu, N.; Ishihara, N.; Newman, T. H.; Malanga, M. T. *J. Mol. Catal. A* **1998**, *128*, 167.
(4) Review: Ewart, S. W.; Baird, M. C. *Metallocene Based Polyolefins, Preparation, Properties and Technology*; Scheirs, J., Kaminsky, W., Ed.; John Wiley & Sons: New York, 2000; Vol. 1, p 119.
(5) Review: Ewart, S. W.; Baird, M. C. *Top. Catal.* **1999**, *7*, 1.
(6) Review: Pellecchia, C.; Grassi, A. *Top. Catal.* **1999**, *7*, 125.
(7) Review: Po, R.; Cardi, N. *Prog. Polym. Sci.* **1996**, *21*, 47.
(8) Review: Vittoria, V. In *Handbook of Thermoplastics*; Olabisi, O., Ed.; Marcel Dekker: New York, 1997; p 81.
(9) Chien, J. C. W.; Salajka, Z. *J. Polym. Sci., Part A: Polym. Chem.* **1991**, *29*, 1243.
(10) Chien, J. C. W.; Salajka, Z. *J. Polym. Sci., Part A: Polym. Chem.* **1991**, *29*, 1253.
(11) Kaminsky, W.; Lenk, S. *Macromol. Symp.* **1997**, *118*, 45.
(12) Kaminsky, W.; Lenk, S.; Scholz, V.; Roesky, H. W.; Herzog, A. *Macromolecules* **1997**, *30*, 7647.
(13) Schneider, N.; Prosenc, M.-H.; Brintzinger, H.-H. *J. Organomet. Chem.* **1997**, *545*, 291.
(14) Xu, G. X.; Ruckenstein, E. *J. Polym. Sci., Part A: Polym. Chem.* **1999**, *37*, 2481.

(15) Foster, P.; Chien, J. C. W.; Rausch, M. D. *Organometallics* **1996**, *15*, 2404.
(16) Quyoum, R.; Wang, Q.; Tudoret, M.-J.; Baird, M. C.; Gillis, D. J. *J. Am. Chem. Soc.* **1994**, *116*, 6435.
(17) Pellecchia, C.; Longo, P.; Proto, A.; Zambelli, A. *Makromol. Chem., Rapid. Commun.* **1992**, *13*, 265.
(18) Ammendola, P.; Pellecchia, C.; Longo, P.; Zambelli, A. *Gazz. Chim. Ital.* **1987**, *117*, 65.
(19) Resconi, L.; Cavallo, L.; Fait, A.; Piemontesi, F. *Chem. Rev.* **2000**, *100*, 1253.
(20) Ricci, G.; Bosisio, C.; Porri, L. *Macromol. Rapid. Commun.* **1996**, *17*, 781.
(21) Zambelli, A.; Pellecchia, C.; Oliva, L.; Han, S. *J. Polym. Sci.* **1988**, *26*, 365.
(22) Buschges, U.; Chien, J. C. W. *J. Polym. Sci., Part A: Polym. Chem.* **1989**, *27*, 1525.
(23) Chien, J. C. W.; Salajka, Z.; Dong, S. *Macromolecules* **1992**, *25*, 3199.
(24) Gillis, D. J.; Tudoret, M.-J.; Baird, M. C. *J. Am. Chem. Soc.* **1993**, *115*, 2543.
(25) Kucht, H.; Kucht, A.; Chien, J. C. W.; Rausch, M. D. *Appl. Organomet. Chem.* **1994**, *8*, 393.
(26) Grassi, A.; Pellecchia, C.; Oliva, L.; Laschi, F. *Macromol. Chem. Phys.* **1995**, *196*, 1093.
(27) Grassi, A.; Zambelli, A.; Laschi, F. *Organometallics* **1996**, *15*, 480.
(28) Xu, G.; Lin, S. *Macromolecules* **1997**, *30*, 685.
(29) Grassi, A.; Saccheo, S.; Zambelli, A.; Laschi, F. *Macromolecules* **1998**, *31*, 5588.
(30) Po, R.; Cardi, N.; Abis, L. *Polymer* **1998**, *39*, 959.
(31) Williams, E. F.; Murray, M. C.; Baird, M. C. *Macromolecules* **2000**, *33*, 261.
(32) Grassi, A.; Longo, P.; Proto, A.; Zambelli, A. *Macromolecules* **1989**, *22*, 104.
(33) Zambelli, A.; Pellecchia, C.; Oliva, L.; Longo, P.; Grassi, A. *Makromol. Chem.* **1991**, *192*, 223.
(34) Kaminsky, W.; Park, Y.-W. *Macromol. Rapid Commun.* **1995**, *16*, 343.
(35) Minieri, G.; Corradini, P.; Zambelli, A.; Guerra, G.; Cavallo, L. *Macromolecules* **2001**, *34*, 2459.
(36) Longo, P.; Grassi, A.; A.; P.; Ammendola, P. *Macromolecules* **1988**, *21*, 24.
(37) Pellecchia, C.; Longo, P.; Grassi, A.; Ammendola, P.; Zambelli, A. *Makromol. Chem., Rapid. Commun.* **1987**, *8*, 277.
(38) Zambelli, A.; Longo, P.; Pellecchia, C.; Grassi, A. *Macromolecules* **1987**, *20*, 2035.
(39) Grassi, A.; Pellecchia, C.; Longo, P.; Zambelli, A. *Gazz. Chim. Ital.* **1987**, *117*, 249.
(40) Longo, P.; Proto, A.; Zambelli, A. *Macromol. Chem. Phys.* **1995**, *196*, 3015.
(41) Corradini, L.; Cavallo, L.; Guerra, G. *Metallocene Based Polyolefins, Preparation, Properties and Technology*; Scheirs, J., Kaminsky, W., Ed.; John Wiley & Sons: New York, 2000; Vol. 2, p 3.
(42) Angermund, K.; Fink, G.; Jensen, V. R.; Kleinschmidt, R. *Chem. Rev.* **2000**, *100*, 1457.
(43) Zambelli, A.; Tosi, C. *Adv. Polym. Sci.* **1974**, *15*, 31.
(44) Resconi, L.; Abis, L.; Franciscono, G. *Macromolecules* **1992**, *25*, 6814.
(45) Erker, G.; Fritze, C. *Angew. Chem., Int. Ed. Engl.* **1992**, *31*, 199.
(46) Zambelli, A.; Tosi, C.; Sacchi, C. *Macromolecules* **1972**, *5*, 649.
(47) Zambelli, A.; Locatelli, P.; Rigamonti, E. *Macromolecules* **1979**, *12*, 156.
(48) Zambelli, A.; Allegra, G. *Macromolecules* **1980**, *13*, 42.
(49) Guerra, G.; Corradini, P.; Pucciariello, R. *Macromolecules* **1985**, *18*, 2030.
(50) Corradini, P.; Busico, V.; Guerra, G. In *Olefin Polymerization*; Kaminsky, W., Sinn, H., Ed.; Springer-Verlag: Berlin, 1988; p 337.
(51) Ricci, G.; Porri, L.; Giarrusso, A. *Macromol. Symp.* **1995**, *89*, 383.
(52) Zambelli, A.; Pellecchia, C.; Proto, A. *Macromol. Symp.* **1995**, *89*, 373.
(53) Corradini, P.; Paiaro, G.; Panunzi, A. *J. Polym. Sci., Part. C* **1967**, *16*, 2906.
(54) Stanley, K.; Baird, M. C. *J. Am. Chem. Soc.* **1975**, *97*, 6598.
(55) *ADF 2.3.0, User Manual*; Vrije Universiteit Amsterdam: Amsterdam, 1996.
(56) Baerends, E. J.; Ellis, D. E.; Ros, P. *Chem. Phys.* **1973**, *2*, 41.
(57) Versluis, L.; Ziegler, T. *J. Chem. Phys.* **1998**, *88*, 322.
(58) te Velde, G.; Baerends, E. J. *J. Comput. Phys.* **1992**, *99*, 84.
(59) Fonseca Guerra, C.; Snijders, J. G.; te Velde, G.; Baerends, E. J. *Theor. Chem. Acc.* **1998**, *99*, 391.
(60) Vosko, S. H.; Wilk, L.; Nusair, M. *Can. J. Phys.* **1980**, *58*, 1200.
(61) Becke, A. *Phys. Rev. A* **1988**, *38*, 3098.
(62) Perdew, J. P. *Phys. Rev. B* **1986**, *33*, 8822.
(63) Perdew, J. P. *Phys. Rev. B* **1986**, *34*, 7406.
(64) McQuarrie, D. A. *Statistical Thermodynamics*; Harper & Row: New York, 1973.
(65) Klamt, A.; Schüürmann, G. *J. Chem. Soc., Perkin Trans. 2* **1993**, 799.
(66) Pye, C. C.; Ziegler, T. *Theor. Chem. Acc.* **1999**, *101*, 396.
(67) Chan, M. S. W.; Vanka, K.; Pye, C. C.; Ziegler, T. *Organometallics* **1999**, *18*, 4624.
(68) *ADF 2000, User Manual*; Vrije Universiteit Amsterdam: Amsterdam, 2000.
(69) It is worthwhile to note that the experimental $E_a = RT^2(\partial[\ln k]/\partial T)_p$, is derived from the "Arrhenius equation", $k = A \exp(-E_a/RT)$, while the standard Gibbs energy difference between the transition state of a reaction and the ground state of the reactants, $\Delta^{\ddagger}G$, is calculated from the experimental rate constant k via the conventional form of the absolute rate equation: $\Delta^{\ddagger}G = RT[\ln(k_B/h) - \ln(k/T)]$. Müller, P. Glossary of Terms Used in Physical Organic Chemistry (IUPAC Recommendations 1994). *Pure Appl. Chem.* **1994**, *66*, 1077.

MA002163D